ELSEVIER

Available online at www.sciencedirect.com

SCIENCE DIRECT®

Journal of Computational and Applied Mathematics 182 (2005) 472–486

JOURNAL OF COMPUTATIONAL AND APPLIED MATHEMATICS

www.elsevier.com/locate/cam

Spiral waves on static and moving spherical domains

Faridon Amdjadi*, Jagnnathan Gomatam

School of Computing and Mathematical Sciences, Division of Mathematics, Glasgow Caledonian University, Cowcaddens Road, Glasgow G4 OBA, UK

Received 17 December 2004; received in revised form 22 December 2004

Abstract

The FitzHugh–Nagumo-type model on static and periodically oscillating surface of the sphere is studied. The numerical investigation of the model is performed in both cases and detailed numerical results are presented for the two-arm spiral wave and its rotation on both manifolds. On the static surface, meandering waves are obtained and it is shown that these waves are stable. On the periodically oscillating surface, the initial excitation gives rise to an irregular (chaotic) meandering rotation, depending on the frequency and the amplitude of the oscillations.

Keywords: FitzHugh–Nagumo-type model; Statics medium; Meandering spiral waves; Stability; Oscillating medium; Chaos

1. Introduction

Wave propagation has been observed in a wide variety of biological and chemical experiments. Examples include un-stirred Belousov–Zhabotinsky (BZ) reaction [22]; BZ chemical waves propagating on the two-dimensional surface of a sphere [16] and cardiac tissues. Mathematical modelling can provide important support and guidance to these experiments. At the simplest level, the electrical activity of the heart can be modelled by a nonlinear reaction–diffusion (RD) equation [21] and the geometry of this wave of electrical activity is governed by the eikonal equation for an anisotropic material [13]. The eikonal equation relates the speed of propagation to the direction of the wave normal

* Corresponding author. Tel.: +44 141 3313618; fax: +44 141 3313608.
E-mail addresses: f.amdjadi@gcal.ac.uk (F. Amdjadi), jgo@gcal.ac.uk (J. Gomatam).

0377-0427/$ - see front matter © 2005 Elsevier B.V. All rights reserved.
doi:10.1016/j.cam.2004.12.027

and to the local curvature at the wave front. A detailed study of this equation on curved manifolds made in [11,12,17,18] highlighted unusual wave forms that are likely to occur in the full RD system. In an excitable media, such as the Belousov–Zhabotinsky reagent, the most striking phenomena is the occurrence of spiral waves [19]. Gomatam and Grindrod consider spiral waves on nonplanar surfaces [11,12] and the same study led to experimentally verifiable predictions [16]. Later, many papers were published on the evolution of spiral waves on circular domains and spherical surface [26,25].

There have been a number of studies regarding motion of spiral waves. Winfree [21,20] was the first to point out that spiral waves observed in two-dimensional excitable media, such as the Belousov–Zhabotinsky chemical reaction, may not rotate periodically around a fixed centre and that the tips of spiral waves may perform complex rotation.

Barkley et al. [7,6,4,14,15] have made the detailed study of core meandering by considering the reaction–diffusion system on the plane. For many choices of system parameters, the tip of the spiral wave executes complicated motion as the spiral rotates. Now, this is well confirmed both in experiments [16] and in fully resolved numerical simulation of two-dimensional media [26,6].

In a previous paper [10], the FitzHugh–Nagumo-type model on the surface of a sphere with fixed radius is considered. The objective of the current paper is as follows:

(i) To further develop and extend the problem considered in [10], by focusing on rotating spirals on static and moving spherical domains. By the numerical integration of the model a two-armed spiral wave, with the two tips, is emerged from a small initial excitation. Two types of modulated waves are obtained, which is due to the variation of the system parameter a. The full description of these waves is given in Section 2 in which we show that for $a = 0.83$ each tip of the spiral meanders on the different hemispheres and traces out a circular helix along the specific latitude of the sphere. Different type of modulation is obtained for $a = 0.55$.

(ii) The unique idea of the paper and of fundamental importance is the study of the stability of meandering spiral waves. Until now there is no mathematical evidence for stability of these waves. As we shall see, these waves are stable by perturbing the solutions from their original position and performing a numerical approach on the resulting equations.

(iii) The innovative feature of the work is related to the size of the excited region; it is shown that the size of the excited region increases after each rotation of the spiral wave, by measuring the distances of the tips from the north-pole. It is also shown that when the spiral length is maximum, the meandering core moves along a specific latitude.

(iv) We also focus on the wave propagation on excitable media that are influenced by geometrical features. Such systems are common in nature and the propagation of electrochemical waves in the heart is an especially important example. It is known that factors such as topology, thickness, and inhomogeneity of cardiac tissue can strongly influence wave propagation and give rise to fibrillation or flutter. We consider wave propagation on the oscillating medium and show that the dynamics of meandering waves change dramatically when the amplitude of the oscillations is varied.

The plan of the paper is as follows: In Section 2, we set up the model and analyse the spiral rotation on a sphere with a fixed radius. In Section 3, we consider the stability of meandering waves. Section 4 is devoted to the analysis of waves in an oscillatory medium, and finally in Section 5, we discuss the overall results that are obtained in this paper with their implication in real world.

2. Setting up the equations: the static medium

The reaction–diffusion equations that we consider is the FitzHugh–Nagumo-type model on the surface of a static sphere:

$$\begin{aligned}\frac{\partial u}{\partial t} &= \nabla_1^2 u + \frac{1}{\varepsilon} f(u, v),\\ \frac{\partial v}{\partial t} &= g(u, v),\end{aligned} \tag{1}$$

where $f = u(1-u)(u - \frac{v+b}{a})$, and $g = u - v$ are nonlinear functions of the variables $u = u(\theta, \phi, t)$, $v = v(\theta, \phi, t)$, and the Laplacian is defined as

$$\nabla_1^2 u = \frac{1}{r^2 \sin\theta} \frac{\partial}{\partial\theta}\left(\sin\theta \frac{\partial u}{\partial\theta}\right) + \frac{1}{r^2 \sin^2\theta} \frac{\partial^2 u}{\partial\phi^2}.$$

The periodicity conditions are

$$\begin{aligned}u(\theta, 0) &= u(\theta, 2\pi) \quad \forall t,\\ v(\theta, 0) &= v(\theta, 2\pi) \quad \forall t.\end{aligned}$$

The excitable medium is a spherical domain and any point in this medium can be defined by the set of co-ordinates $\theta \in [0, \pi]$, $\phi \in [0, 2\pi]$, and $r =$ constant. The Laplacian is singular at $\theta = 0$ and $\theta = \pi$. This can be dealt with as follows: At the poles we have $u(\theta, \phi, t) = u(\theta, \phi + \alpha, t)$ for any real α, which implies that $u(\theta, \phi, t) =$ constant and therefore, at $\theta = 0$ and π, the equations (1) can be written as

$$\begin{aligned}\frac{\partial u}{\partial t} &= \frac{1}{r^2 \sin\theta} \frac{\partial}{\partial\theta}\left(\sin\theta \frac{\partial u}{\partial\theta}\right) + \frac{1}{\varepsilon} f(u, v),\\ \frac{\partial v}{\partial t} &= g(u, v).\end{aligned} \tag{2}$$

Multiplying the first equation of (2) to $\sin\theta$ and setting $\theta = 0$ or $\theta = \pi$ implies $u_\theta = 0$. Therefore at the poles equations (1) can be written as

$$\begin{aligned}\frac{\partial u}{\partial t} &= \frac{1}{r^2} \frac{\partial^2 u}{\partial\theta^2} + \frac{1}{\varepsilon} f(u, v),\\ \frac{\partial v}{\partial t} &= g(u, v).\end{aligned}$$

Although the sphere is a domain with no boundary, however, $u_\theta = 0$ can be considered as Neumann condition at the poles. We discretize the spherical domain as $\theta_i = ih, i = 1, \ldots, 90$ and $\phi_j = jk, k = 1, \ldots, 180$ with $k = h = \frac{\pi}{90}$ and solve the above system (1) by the explicit Euler's method (centred space and forward time). The Laplacian is evaluated by the five-point finite differences approximation. The first- and the second-derivatives are approximated by the following first and the second-order finite

differences formulae:

$$\left(\frac{\partial u}{\partial t}\right)_{i,j} = \frac{1}{\Delta t}\delta_t u_{ij}^{n+1/2} + \mathrm{O}(\Delta t),$$
$$\left(\frac{\partial^2 u}{\partial \theta^2}\right)_{i,j} = \frac{1}{h^2}\delta_\theta^2 u_{ij}^{n} + \mathrm{O}(h^2),$$
$$\left(\frac{\partial^2 u}{\partial \phi^2}\right)_{i,j} = \frac{1}{k^2}\delta_\phi^2 u_{ij}^{n} + \mathrm{O}(k^2),$$

where $\delta_\theta u_{i,j}^n = u_{i+1/2,j}^n - u_{i-1/2,j}^n$, $\delta_\phi u_{i,j}^n = u_{i,j+1/2}^n - u_{i,j-1/2}^n$, $\delta_t u_{i,j}^n = u_{i,j}^{n+1/2} - u_{i,j}^{n-1/2}$, Δt is time step, and h, k are the grid sizes in θ, ϕ directions, respectively. $u_{i,j}^n$ and $v_{i,j}^n$ are the values of the u and v variables at the nth time step at the grid point (i, j). The only remaining parameters are three system parameters a, b and $\varepsilon \ll 1$. First, we choose $a = 0.55$, $b = 0.01$ and $\varepsilon = \frac{1}{100}$. In this study with the above-reported grid points we choose $r = 10$, to allow sufficient domain for wave propagation as well as to pin down the spiral tip easily. For this choice of r the time step is set to $\mathrm{d}t = \frac{1}{20\,000}$ and hence the spiral tip is traced out easily, defining the tip as the intersection of two contours $u = \frac{1}{2}$ and $f(u = \frac{1}{2}, v) = 0$ [2]. Initially, we set $u = 1.0$ and $v = 0.5$ on the immediate left (right)-hand side of the u excitation along a thin strip from the north-pole to the equator. In spherical surfaces with no boundary, a two-arm spiral, with two tips, emerges and each tip performs its own individual rotation. With the choice of the initial solutions described above, one of the tips rotates on the northern-hemisphere and the other one rotates on the southern-hemisphere. At each rotation the two open arms curl and collide, giving rise to the separation of the spiral to two parts. At the beginning of the rotation, one of the separated parts is a large loop which undergoes self-annihilation near the south-pole and the short remaining part give rise to the formation of new spiral, this is shown in Fig. 1(a) (see [10] for full graphical illustration of the process after one spiral rotation). In each successive rotation and collision the size of the short spiral part increases and the size of the large loop part decreases, comparing to the size of the spiral at the previous rotation, so that the spiral wave reaches to its maximum length after elapse of a long period of time (see Fig. 1(b)). Fig. 1(b) is obtained after several rotations and self-annihilations of the loop shape, it shows a spiral wave with its maximum length for $t = 410$. The small loop is already self-annihilated at the back of the sphere near the south-pole. For $t > 410$ the size of spiral does not increase and the core of spiral moves around the vertical axis of the sphere. There is no physical explanation why the spiral wave should rotate around the vertical axis which is only introduced at the level of numerical algorithm. The direction of movement of the spiral depends on the choice of initial condition, noting that our initial condition is a thin strip from the north-pole to the equator.

The radius of the sphere, states the size of the static medium, is a physical parameter and can be varied for different experiments. For a smaller radius, initial excitation dies out quickly and for a very large radius the spiral breaks up to many spirals (see Fig. 2).

We now consider motion of the tips for $a = 0.55$. At each rotation the tip located on the northern-hemisphere rotates around a core (see Fig. 1(a)) and the core moves towards the north-pole which then moves around the pole (see Fig. 3). The core of the other tip moves towards the southern-hemisphere for $t \leqslant 410$ (see Fig. 3(a)), and then moves along the latitude $\theta = 2.7234$. This is typical for meandering patterns where the open end of spiral moves around a core and core moves along a specific latitude [24].

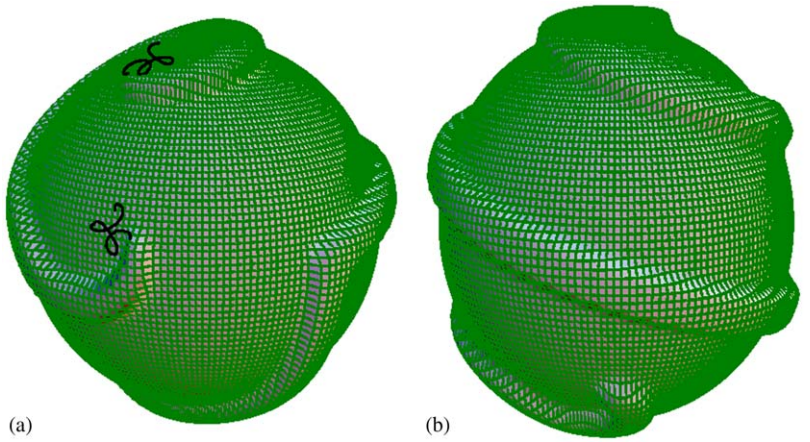

Fig. 1. The physical parameters are $a = 0.55$, $b = 0.01$, $\varepsilon = \frac{1}{100}$. We set $r = 10$, $\Delta t = \frac{1}{20\,000}$ and $h = k = \frac{\pi}{90}$. (a) The initial excitation takes the form of spiral wave and the wave rotates in a meandering fashion. The trajectory of both tips are shown at $t = 3$. The two open arms of the spiral is collided and the wave is separated to two parts. One part is formed a spiral and the other part is formed a large loop which annihilates near the pole. (b) A fully resolved spiral wave with maximum length of excitation is obtained for $t = 410$.

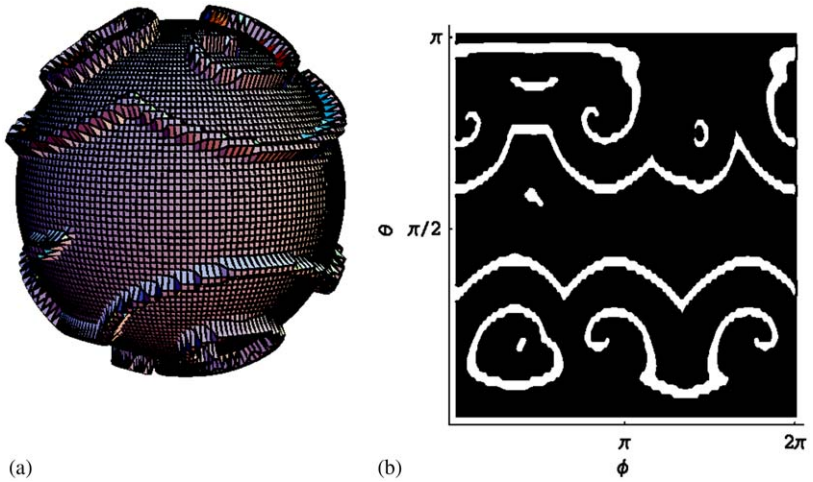

Fig. 2. The physical parameters are $a = 0.55$, $b = 0.01$, $\varepsilon = \frac{1}{100}$, $\Delta t = \frac{1}{20\,000}$ and $h = k = \frac{\pi}{90}$. (a) For $r = 55$ the spiral wave breaks up to many spirals. It is reported that for propagating spiral waves on the plane the spiral wave also breaks to many spirals when the spatial domain of excitation is enlarged [2]. (b) The contour plot of the spiral break up in (ϕ, θ)-plane.

A different scenario is obtained for $a = 0.83$. The initial excitation forms a double-arm spiral wave. In each complete rotation of the spiral wave (i.e., collision and self-annihilation), the spiral tip on the northern-hemisphere rotates around a quasi-periodic core which is a nearly closed loop (i.e., the two ends of the loop do not close completely). The core moves along the latitude $\theta = 0.733411$ tracing out a circular helix shown in Fig. 4 (Barkley [5], refers to this trajectory as modulated waves with infinite

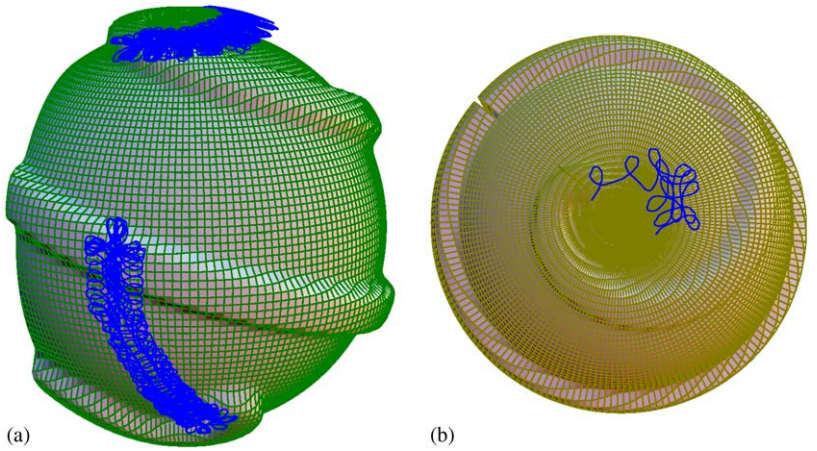

Fig. 3. (a) The trajectories of spiral tips are shown after several rotations at $t = 410$. (b) The spiral and its northern-tip trajectory is viewed from the north-pole for short time interval. For $t > 410$ the core of spiral moves around the pole.

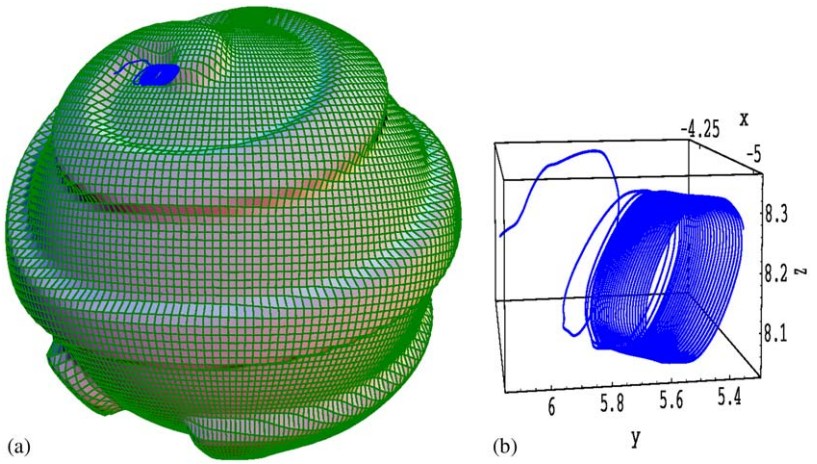

Fig. 4. The parameters are $a = 0.83$, $b = 0.01$, $\varepsilon = \frac{1}{100}$, $\Delta t = \frac{1}{20\,000}$. (a) The tip trace out a quasi-periodic core in each rotation, the core moves along the latitude $\theta = 0.733411$. (b) The trajectory viewed from front for $t \leqslant 70$ and the sphere is not plotted.

period). The tip on the southern-hemisphere trace out a quasi-periodic circular core which first moves towards the south-pole and then moves around the latitude $\theta = 2.27158$ (see Fig. 5).

To clearly understand the tip movement and to find information about the size of the excited region, the distance of the tips from the north-pole is measured at each time step. The distances are the oscillatory functions of time. The distance of southern-tip starts with the uniform and steady oscillations for $t \in (0, 130)$, which then increases for $t \in (130, 535)$ and finally the oscillations remain uniform and steady when the length of spiral is maximum and the core of spiral moves along the latitude $\theta = 2.27158$ (see Fig. 6). Note that the core of the tip on the northern-hemisphere moves along the latitude $\theta = 0.733411$

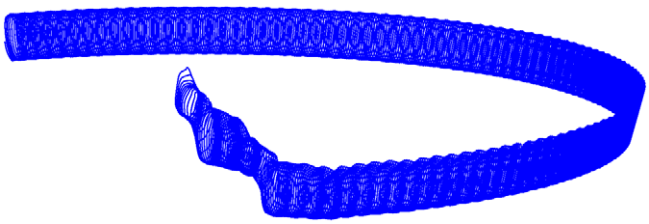

Fig. 5. The tip trajectory of the southern-tip is presented which first moves towards the south-pole and then performs a uniform motion along the latitude $\theta = 2.27158$.

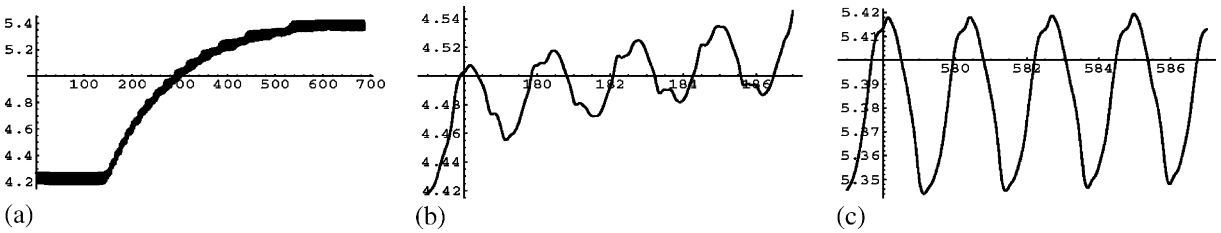

Fig. 6. (a) The south tip's distance from the north-pole for $a=0.83$, $b=0.01$, $\varepsilon=\frac{1}{100}$, $\Delta t=\frac{1}{20\,000}$ is obtained for $t \in [0, 700]$. After the transient dies out, the tip performs uniform oscillations for $t \in (0, 130)$ then it moves towards the southern-hemisphere and the distance increases from the north-pole for $t \in (130, 535)$. Finally, the core of spiral moves around the latitude $\theta = 2.2.27158$ for $t > 535$ giving rise to the uniform and steady oscillations of the tip's distance from the north-pole. The oscillations are shown for a long time period $t \in [0, 700]$, and therefore the graph appears to be a solid thick line. (b) The oscillations are shown in a shorter time period and it is increasing function of time. (c) The oscillations are shown for a shorter time period and for $t > 535$. The oscillations are uniform and periodic.

and therefore its distance from the pole performs steady and uniform oscillations as shown in Fig. 6(c) but in different scale.

3. The stability of meandering waves

In this section we focus on the stability of meandering spiral waves. The stability of a single periodically rotating wave, in a two-dimensional planar excitable medium, analysed in [3]. Barkley [3] transforms the equations to a steady-state problem which supports periodic rotating wave solutions (i.e. the tip is circular), and studies the eigenvalues of the Jacobian matrix calculated at rotating waves. For quasi-periodic solutions, the approach adopted in [3] is not applicable. Our stability analysis of these waves is as follows: Assume $U = U(\theta, \phi, t)$ and $V = V(\theta, \phi, t)$ are the known quasi-periodic solutions of the system (1). We perturb these solutions as

$$\begin{aligned} u(\theta, \phi, t) &= U(\theta, \phi, t) + p(\theta, \phi, t), \\ v(\theta, \phi, t) &= V(\theta, \phi, t) + q(\theta, \phi, t), \end{aligned} \tag{3}$$

where p and q are the small perturbation terms. It is reasonable to see what happens to these perturbations, since the question of stability is whether such (small) disturbances grow or not? Substituting (3)

into (1) gives

$$\frac{\partial U}{\partial t}+\frac{\partial p}{\partial t}=\nabla_1^2(U+p)+\frac{1}{\varepsilon}f(U+p,V+p),$$
$$\frac{\partial V}{\partial t}+\frac{\partial q}{\partial t}=g(U+p,V+q). \tag{4}$$

Expanding the nonlinear functions f and g to the Taylor series about $(U(\theta,\phi,t),V(\theta,\phi,t))$ gives

$$\frac{\partial U}{\partial t}+\frac{\partial p}{\partial t}=\nabla_1^2U+\nabla^2p+\frac{1}{\varepsilon}\left(f(U,V)+\frac{\partial f(U,V)}{\partial u}p+\frac{\partial f(U,V)}{\partial v}q+\mathrm{HOT}\right),$$
$$\frac{\partial V}{\partial t}+\frac{\partial q}{\partial t}=g(U,V)+\frac{\partial g(U,V)}{\partial u}p+\frac{\partial g(U,V)}{\partial v}q+\mathrm{HOT}. \tag{5}$$

Hence, we derive the following truncated linear system of equations:

$$\frac{\partial p}{\partial t}=\nabla_1^2p+\frac{1}{\varepsilon}\left(\frac{\partial f(U,V)}{\partial u}p+\frac{\partial f(U,V)}{\partial v}q\right),$$
$$\frac{\partial q}{\partial t}=p-q, \tag{6}$$

where $\frac{\partial f(U,V)}{\partial u}=(1-U)(U-\frac{V+b}{a})-U(U-\frac{V+b}{a})+U(1-U)$ and $\frac{\partial f(U,V)}{\partial v}=-\frac{1}{a}U(1-U)$. The stability of the solutions $U(\theta,\phi,t)$ and $V(\theta,\phi,t)$ depend on the behaviour of functions p and q, i.e. the solutions are asymptotically stable (or stable) if p and $q\longrightarrow 0$ (or these perturbations remain small with time progression). We analyse this behaviour by solving the linear system (6) numerically. The numerical scheme which we use to solve Eq. (6) is same as the scheme given in the previous section for solving (1) with the parameters $a=0.83$, $b=0.01$, $\varepsilon=\frac{1}{100}$, $\Delta t=\frac{1}{20\,000}$ and $r=10$. Note that the first equation in (6) also depends on the time-dependent solutions $U(\theta,\phi,t)$ and $V(\theta,\phi,t)$. We do not have analytical hold of these solutions and while we are solving Eq. (6), these solutions should be available at each time step. Therefore, to solve (6), the following algorithm is developed:

Step 1: The initial solutions $U_0=U(\theta,\phi,t_0)$, $V_0=V(\theta,\phi,t_0)$, $p_0=U_0/10$ and $q_0=V_0/10$ are given where t_0 is an initial time for which U and V are known. The perturbations p and q are initially small with the norms $\|p_0\|^2=\frac{1}{2\pi}\int_0^{2\pi}|p_0(\theta,\phi,t_0)|^2\,\mathrm{d}\phi=0.6499$, $\|q_0\|^2=\frac{1}{2\pi}\int_0^{2\pi}|q_0(\theta,\phi,t_0)|^2\,\mathrm{d}\phi=0.5842$ at $\theta=\frac{\pi}{4}$.

Step 2: Use U_0 and V_0 to calculate the terms $\frac{\partial f(U,V)}{\partial u}$ and $\frac{\partial f(U,V)}{\partial v}$.

Step 3: Use p_0, q_0 and the partial derivatives calculated in Step 2 and solve (6) for p and q at the next time step. Set the new solutions as p_1 and q_1.

Step 4: Use U_0 and V_0 and solve (1) for u and v at the next time step. Set new solutions as u_1 and v_1.

Step 5: Set $U_0=u_1$, $V_0=v_1$, $p_0=p_1$, $q_0=q_1$ and repeat the Steps 2–4.

We solve the system (6), considering the above algorithm and illustrate the numerical solutions of the function p in Fig. 7. This figure suggests that the oscillations of the function p remain bounded and small. In conclusion, we developed a rigorous and general numerical algorithm for solving the linear equations (6), assuring that the meandering waves are stable.

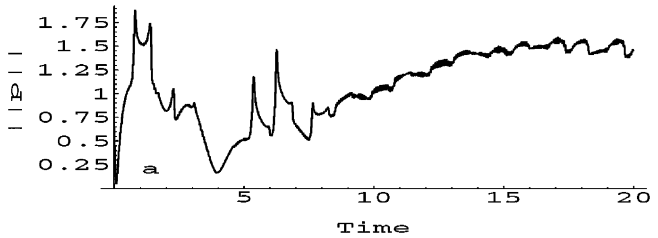

Fig. 7. $\|p\|^2 = \frac{1}{2\pi}\int_0^{2\pi} |p(\frac{\pi}{4}, \phi, t)|^2 \, \mathrm{d}\phi$ with the initial norm $\|p\| = 0.649877$. The oscillations remains bounded and small, i.e. the small disturbance does not grow in time.

4. The moving domain: setting up the equations

In this section, we consider wave propagation on the surface of an oscillating sphere. Biktashev et al. [8] considered wave propagation when the excitable medium is moving with relative shear and they showed that the wave of excitation may be broken by the motion, they considered the planar waves. Here, we consider Eq. (1) on the surface of an oscillating sphere. In such mediums the radius of the sphere, $r = r(t)$, is a periodic function of time. The reaction–diffusion equations on the spherical co-ordinate system, in general, are in the form of

$$\begin{aligned} \frac{\partial u}{\partial t} &= \frac{2}{r}\frac{\partial u}{\partial r} + \frac{\partial^2 u}{\partial r^2} + \nabla_1^2 u + \frac{1}{\varepsilon} f(u, v), \\ \frac{\partial v}{\partial t} &= g(u, v), \end{aligned} \tag{7}$$

where ∇_1, f and g are defined in Section 2. We have

$$\begin{aligned} \frac{\partial u}{\partial t} &= \dot{r}\frac{\partial u}{\partial r}, \\ \frac{\partial^2 u}{\partial t^2} &= \frac{\partial^2 u}{\partial r^2}\dot{r}^2 + \frac{\partial u}{\partial r}\ddot{r}. \end{aligned}$$

Therefore Eq. (7) becomes

$$\begin{aligned} \left(1 - \frac{2}{r\dot{r}} + \frac{\ddot{r}}{\dot{r}^3}\right)\frac{\partial u}{\partial t} &= \frac{1}{\dot{r}^2}\frac{\partial^2 u}{\partial t^2} + \nabla_1^2 u + \frac{1}{\varepsilon} f(u, v), \\ \frac{\partial v}{\partial t} &= g(u, v). \end{aligned} \tag{8}$$

The first equation of (8) is singular for $\dot{r} = 0$. Multiplying this equation by $\dot{r}^3$ and then setting the term $\dot{r}$ to zero implies that $\ddot{r}\frac{\partial u}{\partial t} = 0$. In this work we choose $r(t) = r_0 - A\cos^2 \omega t$, where ω is the frequency of oscillations, A is the amplitude of the oscillations and r_0 is a fixed constant. This choice of r implies that $\ddot{r} \neq 0$ and thus, for $\dot{r} = 0$, the first equation of (8) reduces to $\frac{\partial u}{\partial t} = 0$. For $\dot{r} \neq 0$ the second derivative with respect to time in Eq. (8) can be eliminated as follows: the numerical scheme for Eq. (8) can be

written as

$$\left(1-\frac{2}{r\dot{r}}+\frac{\ddot{r}}{\dot{r}^3}\right)\frac{(u^{n+1}(i,j)-u^n(i,j))}{\Delta t}$$
$$=\frac{1}{\dot{r}^2}\frac{(u^{n+1}(i,j)-2u^n(i,j)+u^{n-1}(i,j))}{\Delta t^2}+\nabla_1^2u^n(i,j)+\frac{1}{\varepsilon}f(u^n(i,j),v^n(i,j)),$$
$$v^{n+1}(i,j)=\Delta t(u^n(i,j)-v^n(i,j)). \tag{9}$$

The first equation of (9) can be rearranged in the following form:

$$\left(1-\frac{2}{r\dot{r}}+\frac{\ddot{r}}{\dot{r}^3}\right)(u^{n+1}(i,j)-u^n(i,j))$$
$$=\frac{1}{\dot{r}^2}\left[\frac{(u^{n+1}(i,j)-u^n(i,j))}{\Delta t}-\frac{(u^n(i,j)-u^{n-1}(i,j))}{\Delta t}\right]$$
$$+\Delta t\left(\nabla_1^2u^n(i,j)+\frac{1}{\varepsilon}f(u^n(i,j),v^n(i,j))\right).$$

In the above equation the term

$$\frac{(u^{n+1}(i,j)-u^n(i,j))}{\Delta t}-\frac{(u^n(i,j)-u^{n-1}(i,j))}{\Delta t}=0,$$

since it consists of the time derivative of the function u at the point (θ_i,ϕ_j), using the forward and the backward differences. Therefore the numerical scheme reduces to the following equations:

$$\left(1-\frac{2}{r\dot{r}}+\frac{\ddot{r}}{\dot{r}^3}\right)(u^{n+1}(i,j)-u^n(i,j))=\Delta t\left(\nabla_1^2u^n(i,j)+\frac{1}{\varepsilon}f(u^n(i,j),v^n(i,j))\right),$$
$$v^{n+1}(i,j)=\Delta t(u^n(i,j)-v^n(i,j)). \tag{10}$$

Now, we choose r_0 and the amplitude of oscillations A so that the spiral wave propagates in time. There exists a critical sphere radius below which spiral waves do not exist. From purely geometrical considerations this critical value r_c can be related to the spiral wavelength λ. An estimated value of r_c can be obtained in the following way: the rotation period, τ, of spiral waves may be found by monitoring the local dynamics at fixed spatial points on the surface of the sphere. Therefore, the wavelength can be obtained from $\lambda=\tau c$ where c is the velocity of the wave propagation which is calculated from the times of excitation of two spatial points separated by a known fixed distance. Thus r_c can be estimated from the condition $\frac{2\pi r_c}{\lambda}\approx 1$, i.e. when the wavelength and the perimeter have the same magnitude.

For the set of parameters chosen in the previous section, i.e., $a=0.83$, $b=0.01$, $\varepsilon=\frac{1}{100}$ and $r=10.0$, our simulation shows that $\tau=2.35$ and $c=24.06$ which implies $r_c=9.0$.

Therefore, with $r_0=10.0$ we choose $A\in[0,1]$. Note that $A=0$ corresponds to the static domain. The radius r depends on the two parameters, i.e. the frequency and the amplitude of the oscillations. First, we fix the frequency of the oscillations at $\omega=15$ and choose a small amplitude $A=0.05$, the parameters are $a=0.83$, $b=0.01$, $\varepsilon=\frac{1}{100}$. With these values we solve Eq. (10), including the case $\dot{r}=0$. The numerical solution is given in Fig. 8. The figure shows that the meandering pattern is oscillating with

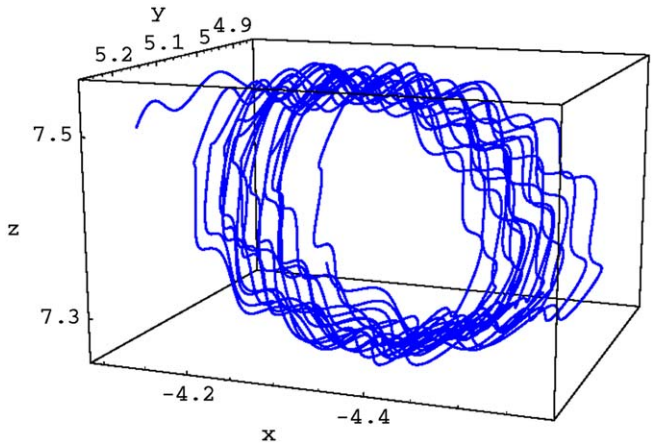

Fig. 8. For $\omega = 15.0$ and $A = 0.05$ the tip trajectory is oscillatory meandering pattern.

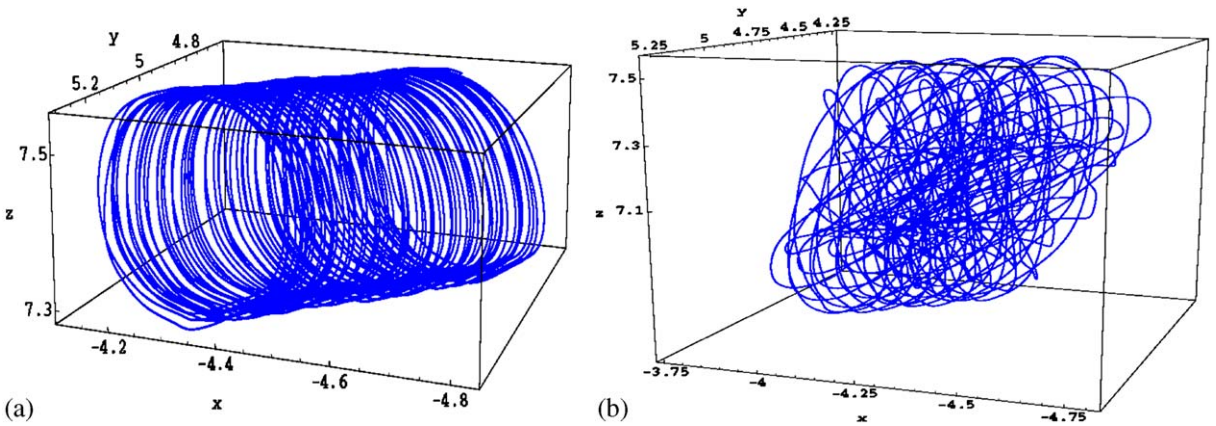

Fig. 9. (a) The trajectory of the tip after several rotations for $A = 0.05$. (b) The trajectory of the tip after several rotations for $A = 0.5$.

respect to the oscillations of the radius r. The dynamics do not change when we increase the amplitude A, only the amplitude of the oscillations shown in Fig. 8 increases. For the higher values of A, say $A = 0.5$, these oscillations collide. Now, we fix the frequency of the oscillations at a lower value $\omega = 1$ and vary the amplitude A in $(0, 1]$, we observe a dramatic change of the dynamics occur at $A = 0.1$. The torus-type modulated wave converts to an erratic modulation shown in Fig. 9. We study closely the change of dynamics by looking at only three rotations and the process is given in Fig. 10. While the motion looks certainly chaotic, the real test lies in how sensitive the motion is to the initial conditions. Therefore we solve Eq. (10) with two, very close, initial solutions say U_c and $U_c + U_c/1000$, where U_c is a known solution, and we monitor the norm of the solutions which is shown in Fig. 11. The oscillations are persistently irregular and never quite settle into a repeating pattern. They display extreme sensitivity

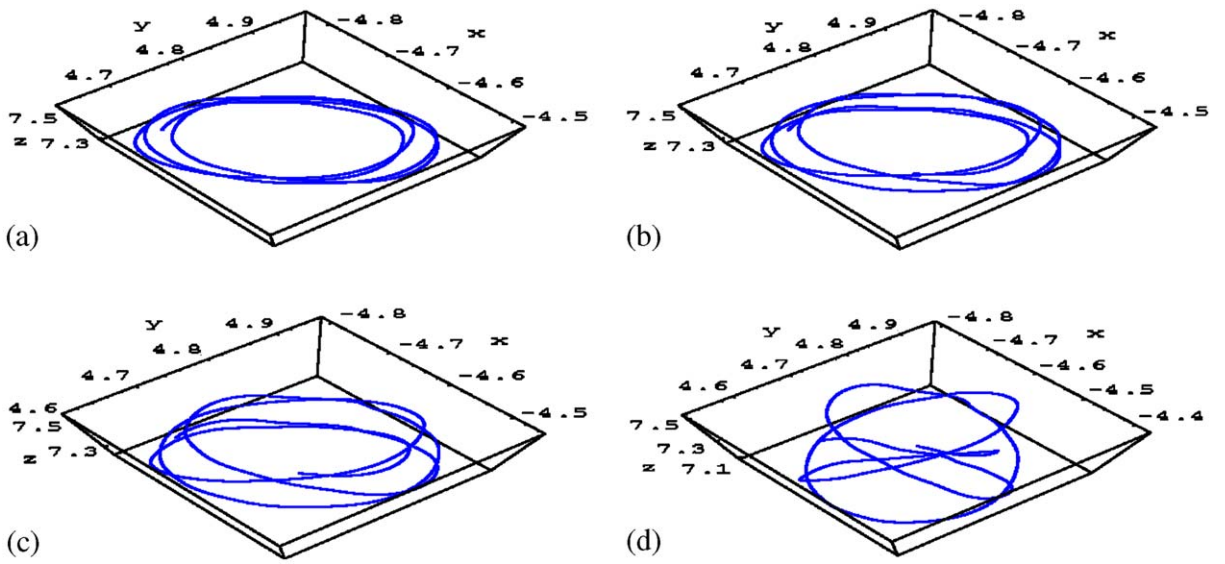

Fig. 10. The parameters are $a = 0.83$, $b = 0.01$, $\varepsilon = \frac{1}{100}$, $\omega = 1$. (a) The trajectory of the tip after 3 rotations for $A = 0.01$. (b) The trajectory of the tip after 3 rotations for $A = 0.05$. (c) The trajectory of the tip after 3 rotations for $A = 0.1$. (d) The trajectory of the type after 3 rotations for $A = 0.3$.

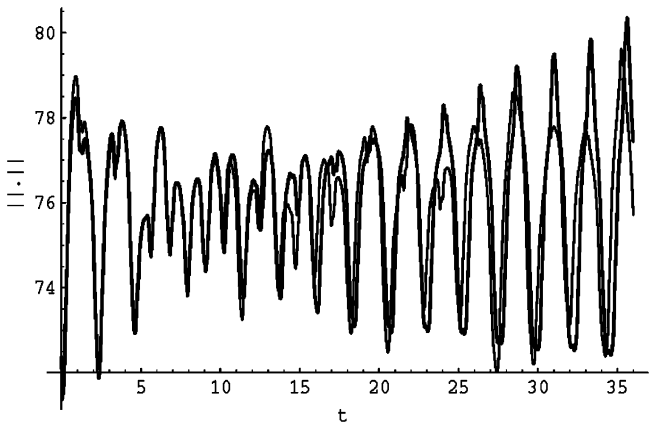

Fig. 11. The light curve is for U and the bold curve is for $U + \frac{U}{100}$.

to initial conditions. The bold curve in Fig. 11 shows the effect of changing the initial condition just 1 part in 1000. At first, the two responses are particularly indistinguishable but after few oscillations the two curves diverges rapidly into two different erratic oscillations. We conclude that a small disturbance on the excitable medium have a major effect on the spiral dynamics and meandering behaviour can convert to an erratic rotation.

5. Discussion

In this paper, we considered spiral waves on a static and an oscillating spherical medium. It is shown that on the static medium, the meandering of spiral waves depends on the physical parameter a. Infinite period waves are obtained for some parameter values and spiral breaking occurred for large domains. It is shown, numerically, that after each rotation of the spiral its length increases until the spiral wave reaches its maximum length and the wave rotates around the vertical axis, due to the choice of initial solutions.

Of fundamental importance is the stability of meandering spiral waves. The stability of rotating waves have been the subject of intensive experimental and theoretical study (see [3] and references therein). Cowie and Rybicki [9] studied the propagation of a detonation wave front in a differentially rotating disk. They derived a partial differential equation and showed that, subject to certain boundary conditions, stable quasi-stationary spiral waves exist which rigidly rotate with a fixed pattern speed. Later Balbus [1] studied the propagating wave on rotating disks and focused on the local inclination of the front, giving some additional insight into the stability of these wave fronts. Balbus [1] focused on the analytical treatment of the partial differential equation. Until now there is no mathematical evidence about the stability of meandering spiral waves. The usual way to study the stability of meandering waves requires the construction of the Monodromy (floquet) matrix and then look for floquet multipliers. This methodology works perfectly for finite-dimensional ordinary differential equations. In this paper, we presented a numerical approach to deal with the time-dependent Jacobian matrix of the linearized equations and to investigate the stability of meandering waves. We considered a small perturbation of a meandering wave from its original position and showed that the perturbation remains bounded and small indicating that the meandering waves are stable.

Geometry often plays a role in determining the nature of pattern structure and dynamics. Our interest is in excitable systems where wave propagation may be strongly influenced by geometrical features. Such systems are common in nature and the propagation of electrochemical waves in the heart is an especially important example. It is known that factors such as topology, thickness, and inhomogeneity of cardiac tissue can strongly influence wave propagation and give rise to fibrillation or flutter. In this paper such complex systems are not considered but instead a much simpler case of excitable medium with spherical oscillatory geometry is examined. Real human hearts are enormously complex three dimensional structures. Although there have been investigations of the dynamics in these complex geometrical domains, in the current study we investigated an extremely simple geometry—a moving spherical geometry. One of our motivations for studying this problem is to develop a mathematical basis for understanding the dynamics of cardiac arrhythmias which are abnormal rhythms in the heart. Although such arrhythmias are most likely associated with changes both in the physiological properties of the tissue as well as the geometry of the tissue, abnormal heart geometries confer significant risk for serious arrhythmia [23]. Thus, it becomes immediately of interest to investigate the possible types of wave organization and their dynamics as a function of the geometry of the excitable medium in which waves propagate.

Part of the motivation for the present study stems from the application of spiral wave dynamics to the physiology of cardiac arrhythmias. Although a real heart is inhomogeneous and has a very complicated geometry and local dynamics, the problems studied here are also of relevance for the heart. In particular, reentrant waves (spiral waves) cause a little movement. It is then important to determine how the movement and geometry changes influence the wave propagation in a moving medium. In the simple moving spherical medium which is studied in this paper the wave propagation is related to the amplitude and frequency of

the oscillations imposed in the medium and dramatic changes in the dynamics of the meandering waves can happen when the amplitude and frequency of the oscillations are varied.

While the topology of a heart is quite complex and differs from that of a simple spherical moving domain, some of the principle features of spiral wave dynamics are best elucidated by studying more simple dynamics in simple geometries, such as the moving spherical domain considered here.

One may extend the understanding of the dynamics presented here to include more complicated models. Examples of such models include spiral oscillation on a moving spherical shell in which case a finite element approach might be a possible approximation.

References

[1] S.A. Balbus, The propagation and stability of time dependent galactodetonation waves, Astrophys. J. 277 (1984) 550–555.
[2] D. Barkley, A model for fast computer simulation of waves in excitable media, Physica D 49 (1991) 61–70.
[3] D. Barkley, Linear stability analysis of rotating spiral waves in excitable media, Phys. Rev. Lett. 68 (13) (1992) 2090–2093.
[4] D. Barkley, Euclidean symmetry and the dynamics of rotating spiral waves, Phys. Rev. Lett. 72 (1) (1993) 164–167.
[5] D. Barkley, Euclidian symmetry and the dynamics of rotating spiral waves, Phys. Rev. Lett. 72 (1) (1993) 164–176.
[6] D. Barkley, I.G. Keverkidis, A dynamical system approach to spiral wave dynamics, Chaos 4 (1994) 453–460.
[7] D. Barkley, M. Kness, S. Tuckerman, Spiral-wave dynamics in a simple model of excitable media: the transition from simple to compound rotation, Phys. Rev. A 42 (1990) 2489–2492.
[8] V.N. Biktashiv, A.V. Holden, M.A. Tsyganov, Excitation wave breaking in excitable media with linear shear flow, Phys. Rev. Lett. 81 (13) (1998) 2815–2818.
[9] L.L. Cowie, G.B. Rybicki, The structure evolution of galacto-detonation waves: some analytic results in sequential formation models of spiral galaxies, Astrophys. J. 260 (1982) 504–511.
[10] J. Gomatam, F. Amdjadi, Reaction–diffusion equations on a sphere: meandering of spiral waves, Phys. Rev. E 56 (4) (1997) 3913–3919.
[11] J. Gomatam, P. Grindrod, Three-dimensional waves in excitable reaction diffusion systems, J. Math. Biol. 25 (1987) 611–622.
[12] J. Gomatam, P. Grindrod, The geometry and motion of reaction–diffusion waves on closed two-dimensional manifolds, J. Math. Biol. 25 (1987) 597–610.
[13] J.P. Keener, An eikonal-curvature equation for action potential propagation in myocardium, J. Math. Biol. 29 (1991) 629–651.
[14] R.M. Mantel, D. Barkley, Parametric forcing of scroll-wave patterns in three-dimensional excitable media, Physica D 149 (2000) 107–122.
[15] D. Margerit, D. Barkley, Cookbook asymptotics for spiral and scroll waves in excitable media, J. Chaos 12 (3) (2002) 636–649.
[16] J. Maselko, K. Showalter, Chemical waves on spherical surfaces, Nature 339 (1989) 609–611.
[17] A.J. Mulholland, J. Gomatam, The eikonal approximation to excitable reaction–diffusion systems: travelling non-planar wavefronts on the plane, Physica D 89 (3–4) (1996) 329–345.
[18] A.J. Mulholland, J. Gomatam, P. McQuillan, Diffraction of spherical waves by a toroidal obstacle: eikonal approach to excitable reaction–diffusion systems, Proc. Roy. Soc. Ser. A 452 (1996) 2785–2799.
[19] B.J. Welsh, J. Gomatam, A.E. Burgess, Three-dimensional chemical waves in the Belousov–Zhabotinsky reaction, Nature 304 (1983) 611–614.
[20] A. Winfree, Spatial and temporal organization in Zhabotinsky reaction, Adv. Biol. Med. Phys. 16 (1973) 115–136.
[21] A. Winfree, When Time Breaks Down, Princeton University Press, Princeton, NJ, 1987.
[22] A.T. Winfree, Spiral waves of chemical activity, Science 175 (1972) 634–636.
[23] D.P. Zipes, J. Jalife (Eds.), Cardiac Electrophysiology. From Cell to Bedside, Saneders, WB, Philadelphia, 1995.

[24] V.S. Zykov, A.S. Mikhailov, S.C. Muller, in: H. Engel, F.J. Niedemostheide, H.G. Purwins, E. Scholl (Eds.), Self-Organization in Activator–Inhibitor Systems: Semiconductors, Gas-Discharge and Chemical Active Media, W&T-Verlage, Berlin, 1996.
[25] V.S. Zykov, A.S. Mikhailov, S.C. Muller, Controlling spiral waves in confined geometries by global feedback, Phys. Rev. Lett. 78 (17) (1997) 3398–3401.
[26] V.S. Zykov, S.C. Muller, Spiral waves on circular and spherical domains of excitable medium, Physica D 97 (1996) 322–332.